



Composition of Mars constrained using geophysical observations and mineral physics modeling



Yi Wang^{a,*}, Lianxing Wen^{b,a}, Donald J. Weidner^b

^aLaboratory of Seismology and Physics of Earth's Interior, University of Science and Technology of China, Hefei, Anhui 230026, China

^bDepartment of Geosciences, State University of New York at Stony Brook, Stony Brook, NY 11794, United States

ARTICLE INFO

Article history:

Received 25 April 2013

Received in revised form 15 July 2013

Accepted 1 August 2013

Available online 21 August 2013

Edited by K. Hirose

Keywords:

Mars composition

Mean moment of inertial

Mineral physics modeling

Density distribution

ABSTRACT

We use the total mass, possible core radius and the observed mean moment of inertia factor of Mars to constrain mineralogical and compositional structures of Mars. We adopt a liquid Fe–S system for the Martian core and construct density models of the interior of Mars for a series of mantle compositions, core compositions and temperature profiles. The moment of inertia factor of the planet is then calculated and compared to the observation to place constraints on Mars composition. Based on the independent constraints of total mass, possible core radius of 1630–1830 km, and the mean moment of inertia factor (0.3645 ± 0.0005) of Mars, we find that Fe content in the Martian mantle is between 9.9 and 11.9 mol%, Al content in the Martian mantle smaller than 1.5 mol%, S content in the Martian core between 10.6 and 14.9 wt%. The inferred Fe content in the bulk Mars lies between 27.3 and 32.0 wt%, and the inferred Fe/Si ratio in Mars between 1.55 and 1.95, within a range too broad to make a conclusion whether Mars has the same nonvolatile bulk composition as that of CI chondrite. We also conclude that no perovskite layer exists in the bottom of the Martian mantle. Based on the inferred density models, we estimate the flattening factor and J_2 gravitational potential related to the hydrostatic figure of the rotating Mars to be $(5.0304 \pm 0.0098) \times 10^{-3}$ and $(1.8151 \pm 0.0065) \times 10^{-3}$, respectively. We also discuss implications of these compositional models to the understanding of formation and evolution of the planet.

© 2013 Elsevier B.V. All rights reserved.

1. Introduction

Compositions of the mantle and the core of the terrestrial planets are important for our understanding of the formation and evolution of the planets. There are two hypotheses on the evolution of the planets. One hypothesis states that the different mean densities of the terrestrial planets indicate different Fe/Si ratios in their bulk composition, which reflects an Fe/Si fractionation in the solar nebula according to the distances the planets are away from the Sun (Urey, 1952; Ganapathy and Anders, 1974). The other hypothesis states that the terrestrial planets all have the bulk composition with the same nonvolatile element abundances as those of CI carbonaceous chondrite (Ringwood, 1959). Later, this hypothesis is revised to be that the terrestrial planets consist of two chondritic components, with one completely reduced and the other oxidized, but both components have the same bulk composition of CI chondrite (Wanke and Dreibus, 1988). Based on this hypothesis, the terrestrial planets would have the same Fe/Si ratio, but different ratios

between metallic Fe and the total Fe. Most geosciences studies conclude that it is possible for Earth to have the same bulk composition as that of chondrite (e.g. Allegre et al., 2001), but some studies suggest a different bulk composition of Earth (e.g. Javoy et al., 2010). Understanding the composition of other terrestrial planets can help us to evaluate these two hypotheses.

One obvious candidate planet is Mars. Many studies analyze the SNC (Shergottites, Nakhilites and Chassigny) meteorites to study bulk composition of Mars, including its major elements (e.g. Dreibus and Wanke, 1985) and isotopes (e.g. Lodders and Fegley, 1997; Sanloup et al., 1999; Mohapatra and Murty, 2003). The bulk compositional models from all these studies suggest that, comparing to Earth, Mars has more FeO in the mantle and more S in the core.

Physical data, such as mass, size, moment of inertia (MOI) factor can also be used to constrain bulk composition of Mars (Anderson, 1972; Mocquet et al., 1996; Bertka and Fei, 1998; Rivoldini et al., 2011). Recent missions to Mars have provided more precise measurements of the MOI factor. Previous study (Bertka and Fei, 1998) uses the polar MOI factor and mineral physics data to constrain Mars composition. The study assumes a solid core and a fixed mantle composition. They conclude that the bulk composition

* Corresponding author. Tel.: +86 551 63600715.

E-mail addresses: yiwang25@ustc.edu.cn (Y. Wang), Lianxing.Wen@sunysb.edu (L. Wen), dweidner@notes.cc.sunysb.edu (D.J. Weidner).

of Mars is different from that of CI chondrite. A recent study, however, has suggested a liquid core in Mars (Yoder et al., 2003). Recent progress in mineral physics now also allows us to quantitatively predict velocity and density profiles for various mantle compositions, core compositions and temperature profiles within the planets (Weidner and Wang, 1998; Wang et al., 2006, 2008, 2009). In this study, we adopt a liquid Fe–S system in the core and test a variety of mantle compositions. Our mineral physics modeling method allows us to systematically search for possible compositions in the mantle and the core. We construct one-dimensional (1-D) density models of the interior of Mars for a series of compositions of the mantle and the core, and calculate the MOI factors. Comparing the calculated MOI factors with the observation, we place constraints on the mantle and core compositions in Mars. We discuss our methods in Section 2, modeling results in Section 3, and the effects of assumed crust model, temperature profile, as well as comparisons to previous studies, predictions of other geophysical parameters and non-existence of a perovskite layer in the bottom of the Martian mantle in Section 4.

2. Method

2.1. Moment of inertia (MOI) factor

MOI factor around a particular rotation axis is defined as $C = \int r^2 dm / MR^2$, where dm is mass integral, r the distance of dm to the rotation axis, M the total mass, and R the mean radius of the planet. Since Mars is not a perfect sphere, the MOI of the planet depends on the choice of axis. The polar MOI factor is the one with respect to the planets rotation axis. The mean MOI factor is defined as $I = \frac{1}{3}(A + B + C)$, where A and B are the principal equatorial MOI factors, and C is the polar MOI factor.

With the knowledge of a planets total mass, the mean radius R and the MOI factor, we can place constraints on density models inside the planet, which can be linked to its composition based on mineral physics modeling. Since our 1-D density models do not include the hydrostatic figures, we should use the inferred mean MOI factor instead of the polar MOI factor. Recent space missions provide us precise measurement of the MOI of Mars. Konopliv et al. (2011) calculate the mean MOI factor of Mars to be 0.3645 ± 0.0005 based on the measurements of Mars Reconnaissance Orbiter, Mars Global Surveyor, Odyssey, Pathfinder and Viking.

2.2. Mineral physics modeling

In mineral physics modeling, density distribution in the Martian mantle are calculated following the procedures outlined in Weidner and Wang (1998), Wang et al. (2006, 2008, 2009). In order to calculate the velocity and density for a certain mantle temperature and composition, we need to know the stable minerals and volume fraction, chemical composition and physical properties of each stable mineral under the condition of the mantle temperature, pressure and composition. We use phase equilibria data to define the stable assemblages at relevant pressures and temperatures, cation distribution data to define the chemical composition of each stable phase. This information, along with our current estimates of physical properties of these phases, provides a mineralogical model with volume fractions of each phase along with aggregate velocities and densities. In this study, we use the phase diagram for the earth upper mantle reported by Gasparik Chapter 10 in (Gasparik, 2003) as a template for defining the evolution of the system through mantle phase transformations, and consider both olivine and garnet components and their chemical interactions. In the phase diagram, we also ignore a low-pressure mineral, Al-rich pyroxene, and a phase transformation from Al-rich pyroxene to

garnet occurring at 2 GPa (about 160 km depth), as the density difference between 50–160 km depth caused by the low-pressure mineral is less than 1%, and has small effect on MOI factor. Since in the mantle, most of Al is in garnet and perovskite, and the Al contents of other minerals are negligible, we assume that all Al is in garnet and perovskite with other minerals Al-free (Gasparik, 1990). For every mineral, we extrapolate their elastic properties to certain pressures and temperatures in the Martian mantle using the third order Birch–Murnaghan equation of state (Birch, 1947). Based on the volume and the mole fraction of every stable mineral, we calculate the volume fraction and density of each stable mineral, and then the combined density of the assemblage.

We use the temperature model from Fei and Bertka (2005) study as a reference temperature profile inside Mars. This reference temperature profile is below the mantle solidus and above the melting temperature of Fe–14.2 wt% S (Bertka and Fei, 1998 Martian core model) but below the melting temperature of pure Fe. So Mars has a solid mantle and a liquid/solid core based on this temperature profile. We also test the effects of different temperature profiles. We use the composition model of Wanke and Dreibus (1988) as a reference mantle composition model (Table 1), and test different Fe contents and Al contents in the Martian mantle. As a recent study (Yoder et al., 2003) suggests that the Martian core is liquid, we adopt a liquid Fe–S system in the Martian core. We calculate core density profiles for various S contents based on the measurements of elastic properties for pure liquid Fe (Anderson and Ahrens, 1994) and for liquid Fe with 10 wt% S (Balog et al., 2003; Sanloup et al., 2000) (Table 2), assuming the elastic properties of the system linearly change with S content. A recent study (Wieczorek and Zuber, 2004) estimates that the average crust thickness of Mars to be between 38 and 62 km, and the crust density between 2.7 and 3.1 g/cm³. In our modeling, a Martian crust with a thickness of 50 km and a density of 3.0 g/cm³ is adopted, but we also test the effects of the crust thickness and density in the reported range of parameters.

We calculate density profiles in the mantle and the core for a series of mantle and core compositions. Fig. 1 shows an example of mineral assemblages (Fig. 1b) and a density profile (Fig. 1a) inside Mars calculated based on Fei and Bertka (2005) temperature model, Wanke and Dreibus (1988) mantle composition model and a liquid Fe–S system with 12 wt% S in the core. For a particular mantle composition, core composition and temperature profile, only one core radius can be inferred to fit the total mass of Mars. For each density model, we calculate the MOI factors and use possible core radius (1630–1830 km) (Konopliv et al., 2011) and the inferred mean MOI factor (0.3645 ± 0.0005) (Konopliv et al., 2011) to place constraints on Mars composition.

3. Modeling results

Density in the Martian core is influenced by its S content. A higher S content results in a lower density in the core, and requires a larger core radius to fit the total mass (Fig. 2a). For a fixed mantle density, a less dense and larger core would result in a larger mean MOI factor. A lower S content would do the opposite (Fig. 2b).

Fe content in the mantle has significant effects on mantle density and the mean MOI factor of Mars. Increasing Fe content would increase the density of every mineral in the mantle. At the same time, increasing Fe content would also result in increasing

Table 1
Reference mantle composition model of Mars (Wanke and Dreibus, 1988).

	MgO	FeO	CaO	SiO ₂	Al ₂ O ₃
Wt%	30.20	17.90	2.45	44.40	3.02
Mol%	40.72	13.54	2.37	40.16	3.21

Table 2
Elastic measurements of liquid Fe–S system.

Material	T (K)	ρ (g/cm ³)	K (GPa)	K'	α (K ⁻¹)
Fe ^a	1811	7.019	85.0 ^b	4.66	9.27×10^{-5}
Fe + 10%S ^c	1923	5.5	63	4.8	9.27×10^{-5d}

^a Anderson and Ahrens (1994).

^b This bulk value is corrected from adiabatic (K_S) to isothermal (K_T) via the relationship $K_T = \frac{K_S}{1 + \alpha T}$.

^c Balog et al. (2003), Sanloup et al. (2000).

^d This thermal expansion coefficient is not available. We assume 10 wt% sulfur would not cause a significant change in thermal expansion, and use a constant thermal expansion coefficient of 9.27×10^{-5} .

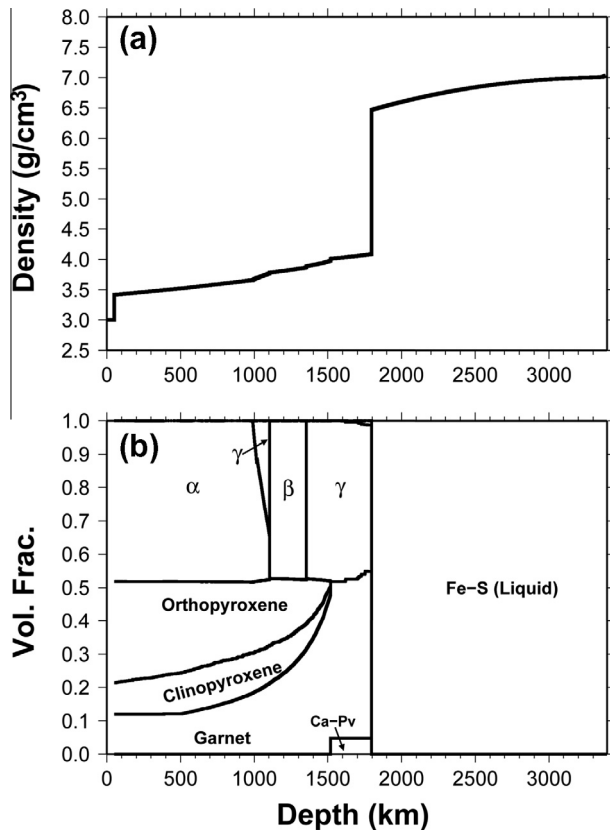


Fig. 1. Calculated density profile (a) and volume fractions of various minerals (b) in the interior of Mars, based on the temperature model of Fei and Bertka (2005), the mantle composition model of Wanke and Dreibus (1988) and a liquid Fe–S core with 12 wt% S. A Martian crust with a thickness of 50 km and a density of 3.0 g/cm³ is adopted. α denotes olivine; β wadsleyite; γ ringwoodite; and Ca–Pv, Calcium-perovskite.

olivine/pyroxene ratio, since Fe varies with all other cations being in fixed molar proportions. The effect of changing olivine/pyroxene ratio on mantle density is smaller than the effect of Fe content on the density of every mineral of the assemblage. Overall, a higher Fe content results in a higher density in the mantle (Fig. 3). If the core density is fixed, increasing mantle density would require a decreasing core radius to fit the total mass of Mars (Fig. 2a). A higher mantle density and a smaller core radius would result in a higher mean MOI factor. A higher Fe content in the Martian mantle would result in a smaller core radius (Fig. 2a) and a higher mean MOI factor (Fig. 2b) of Mars, when the core composition is fixed. We search a series of composition models with different Fe contents (the molar ratios between other elements are fixed) in the mantle and different S contents in the core (Fig. 2). With the constraints of the total mass, possible core radius (1630–1830 km) and the inferred mean MOI factor (0.3645 ± 0.0005), we find that Fe

content in the Martian mantle is between 9.9 and 11.9 mol% (shaded region in Fig. 2b), and S content in the Martian core between 10.6 and 14.9 wt% (shaded region in Fig. 2b).

Al content does not affect the elastic properties of mantle minerals significantly, but it influences the stability of garnet. So the Al content also affects the mantle density and the mean MOI factor of Mars. A higher Al content would make garnet more stable, resulting in more garnet and less pyroxene in the mantle. Garnet has a larger density than that of pyroxene, so increasing Al content in the mantle would increase mantle density (Fig. 4). If the core composition is fixed, an increasing Al content in the mantle requires a decreasing core radius (Fig. 5a) and results in a higher mean MOI factor (Fig. 5b). We search a series of composition models with different Al contents (the molar ratios between other elements are fixed) in the mantle and various S contents in the core (Fig. 5). With the constraints of the total mass, possible core radius and the inferred mean MOI factor, we find that Al content in the Martian mantle is smaller than 1.5 mol% (shaded region in Fig. 5b), and S content in the Martian core between 10.6 and 14.9 wt% (shaded region in Fig. 5b).

For these possible mantle and core composition models, we calculate the bulk Fe content and the Fe/Si ratio in Mars (Tables 3–6), including the four end members A, B, C, D in Fig. 2b (Lines 1–4 in Table 3) and the three end members A, B, C in Fig. 5b (Lines 1–3 in Table 4). In the possible composition range, if S content in the core is fixed, either an increasing Fe content (Lines 5–6 in Table 3) or an increasing Al content (Lines 4–5 in Table 4) in the mantle would result in a decreasing core radius, a decreasing total Fe content and a decreasing Fe/Si ratio in Mars. If mantle composition is fixed, an increasing S content in the core would result in an increasing core radius, an increasing total Fe content and an increasing Fe/Si ratio in Mars (Lines 1–3 in Table 5). Based on the constraints of the total mass, possible core radius and the inferred mean MOI factor, the total Fe content in Mars is between 27.3 and 32.0 wt%, and the Fe/Si ratio in Mars is between 1.55 and 1.95 (Point C in Fig. 2b, Point B in Fig. 5b, Line 3 in Table 3, Line 2 in Table 4). CI carbonaceous chondrite has an Fe content of 27.8 wt% and an Fe/Si ratio of 1.71 (Line 12 in Table 3), which are within our possible composition range. However, our possible composition range is not narrow enough to make a conclusion whether Mars has the same nonvolatile element abundances as those of CI carbonaceous chondrite. During our modeling, when we test different Fe contents in the Martian mantle, we have kept Al content in the mantle the same as that of Wanke and Dreibus (1988) mantle composition model, and vice versa. If we allow Fe and Al contents both to vary, the possible composition range would be even broader. The Mg# of different Martian mantle models does not change much in our possible composition range, lying between 41.4 and 41.6 mol%.

4. Discussion

4.1. Effect of the Martian crust thickness and density

In our modeling, we used a fixed Martian crust model with a thickness of 50 km and a density of 3.0 g/cm³. Crust thickness and density have effects on MOI factor and the inferred core radius. For a certain mantle and core composition model, either a larger crust thickness or a smaller crust density would require a larger core radius to fit the total mass (Fig. 6a), and result in a smaller MOI factor (Fig. 6b). A thicker crust or a less dense crust would require a high bulk Fe content and a high Fe/Si ratio in Mars to fit the constraint of MOI factor (Fig. 7, Lines 1–4 in Table 6). Our inferred Martian composition range (the total Fe content between 27.3 and 32.0 wt%; the Fe/Si ratio between 1.55 and 1.95) is based on our reference crust model (thickness = 50 km, density = 3.0 g/cm³). A recent study shows that the Martian crust thickness is between

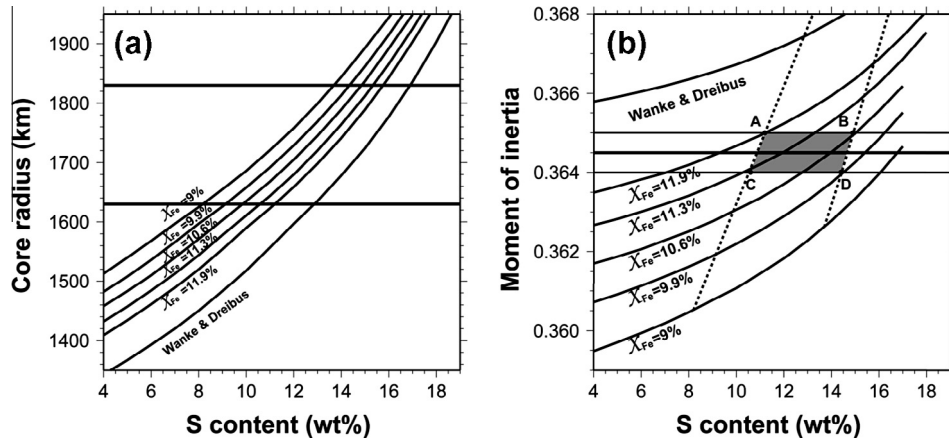


Fig. 2. Calculated core radius (a) and MOI factor (b) as a function of S content in the core for various Fe contents (X_{Fe}) in the mantle. A Martian crust with a thickness of 50 km and a density of 3.0 g/cm^3 is adopted. The solid lines in (a) and the dashed lines in (b) are the range of possible core radius, 1630 km and 1830 km inferred by Konopliv et al. (2011); the solid lines in (b) are the observed value and error bars of the mean MOI factor.

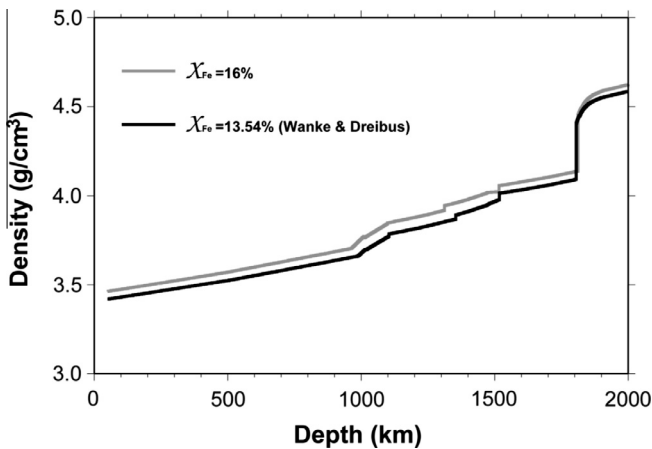


Fig. 3. Calculated mantle density profiles inside Mars based on two composition models with an Fe content (X_{Fe}) of 16 and 13.54 mol%, respectively.

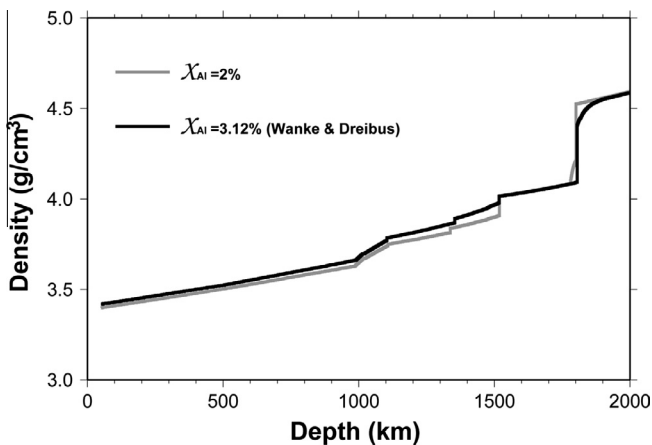


Fig. 4. Calculated mantle density profiles inside Mars based on two composition models with an Al content (X_{Al}) of 2 and 3.12 mol%, respectively.

38 and 62 km, and the crust density is between 2.7 and 3.1 g/cm^3 (Wieczorek and Zuber, 2004), so we consider two end members: a Martian crust (1) with a thickness of 62 km and a density of 2.7 g/cm^3 ; (2) with a thickness of 38 km and a density of 3.1 g/cm^3 and a fix Al content in the Martian mantle. With the

end member 1, Fe content in the Martian mantle is inferred to be between 12.0 and 13.9 mol%, S content in the Martian core between 11.5 and 15.6 wt%, the total Fe content between 28.2 and 30.6 wt%, and the Fe/Si ratio between 1.64 and 1.88 (Fig. 7a, Lines 1–4 in Table 6). With the end member 2, Fe content in the Martian mantle is inferred to be between 9.3 and 11.2 mol%, S content in the Martian core between 10.2 and 14.7 wt%, the total Fe content between 26.9 and 29.3 wt%, and the Fe/Si ratio between 1.52 and 1.75 (Fig. 7b, Lines 5–8 in Table 6). If we allow the crust thickness and density to vary within Wieczorek and Zuber (2004) Martian crust model range (38–62 km, 2.7 – 3.1 g/cm^3), the possible composition range becomes broader and it does not change our conclusion on whether Mars has the same nonvolatile bulk composition as that of CI chondrite.

With our reference crust model, Wanke and Dreibus (1988) composition model is not a plausible mantle composition model for Mars to fit the constraint of mean MOI (0.3645 ± 0.0005) (Fig. 6), but a thicker or less dense crust could reduce the MOI value and make the composition model plausible for the Martian mantle (Fig. 6).

4.2. Temperature effect

Temperature effect on the inferred core radius and MOI is not significant. For a certain mantle and core composition model, a mantle temperature difference of 100 K would result in 2–3 km difference in core radius and less than 0.05% difference in MOI factor, while a core temperature difference of 100 K would result in 3–7 km difference in core radius and less than 0.02% difference in MOI factor. A temperature deviation of a few hundred K from the reference profile does not alter the conclusions of this study.

4.3. Comparisons to previous study

Our study concludes that the total Fe content in Mars is between 27.3 and 32.0 wt%, the Fe/Si ratio in Mars is between 1.55 and 1.95, and the possible composition range is too broad to make a conclusion if Mars has the same nonvolatile bulk composition as that of CI chondrite (Fe% = 27.8 wt%, Fe/Si = 1.71, Lines 12 in Table 3). The results are different from the conclusion of the study of Bertka and Fei (1998) that the total Fe content and the Fe/Si ratio in Mars (Fe% = 23.1 wt%, Fe/Si = 1.319, Lines 11 in Table 3) are smaller than those of CI chondrite.

The different conclusions between the two studies are due to four factors. (1) We adopt a liquid Fe–S system in the core, while

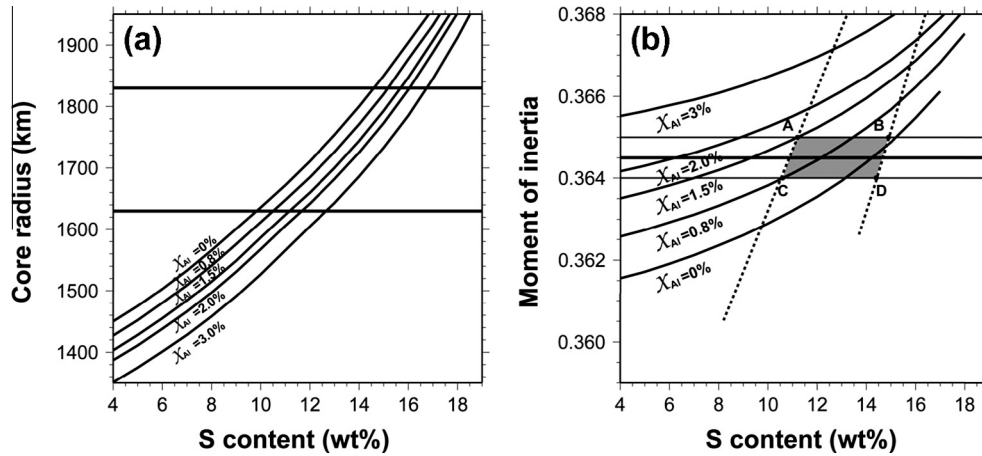


Fig. 5. Calculated core radius (a) and MOI factor (b) as a function of S content in the core for various Al contents (X_{Al}) in the mantle. A Martian crust with a thickness of 50 km and a density of 3.0 g/cm^3 is adopted. The solid lines in (a) and the dashed lines in (b) are the range of possible core radius, 1630 km and 1830 km inferred by [Konopliv et al. \(2011\)](#); the solid lines in (b) are the observed value and error bars of the mean MOI factor.

Table 3
Composition of Mars for various Fe contents in the mantle and S contents in the core.

No	Mantle model (mol%)	S in Core (wt%)	Core radius (km)	Bulk Fe (wt%)	Fe/Si
1	Fe = 11.9	11.2	1630	24.7	1.56
2	Fe = 10.6	14.9	1832	29.7	1.78
3	Fe = 11.3	10.6	1630	27.3	1.55
4	Fe = 9.9	14.4	1832	29.5	1.76
5	Fe = 10	11	1688	27.7	1.58
6	Fe = 11	11	1655	27.5	1.57
7	Fe = 13.0	0.0	1283	24.3	1.29
8	Fe = 11.6	10.8	1627	27.3	1.55
9	Fe = 10.3	14.6	1828	29.5	1.77
10	Fe = 0.0	21.1	2552	41.9	3.45
11	BF ^a	14.2	1421	23.1	1.319
12	C1 Chondrite			27.8	1.71

^a Bertka and Fei (1998).

Table 4
Composition of Mars for various Al contents in the mantle and S contents in the core.

No	Mantle model (mol%)	S in Core (wt%)	Core radius (km)	Bulk Fe (wt%)	Fe/Si
1	Al = 1.5	11.2	1631	28.8	1.65
2	Al = 0.2	14.8	1832	32.0	1.95
3	Al = 0.8	10.6	1634	29.2	1.68
4	Al = 0.0	11	1672	30.1	1.74
5	Al = 1.0	11	1841	29.2	1.68
6	C1 Chondrite			27.8	1.71

Table 5
Composition of Mars for [Wanke and Dreibus \(1988\)](#) mantle composition model and various S contents in the core.

No	Mantle model (mol%)	S in Core (wt%)	Core radius (km)	Bulk Fe (wt%)	Fe/Si
1	WD model ^a	0.0	1262	24.2	1.29
2	WD model	7.1	1423	25.4	1.40
3	WD model	14.3	1691	28.4	1.67
4	C1 Chondrite			27.8	1.71

^a [Wanke and Dreibus \(1988\)](#).

[Bertka and Fei \(1998\)](#) used a solid core assumption; (2) we search for all possible ranges of mantle composition, while [Bertka and Fei](#)

Table 6
Composition of Mars for two crust models.

No	Crust model	Mantle model (mol%)	S in Core (wt%)	Core radius (km)	Mcore (wt%)	Bulk Fe (wt%)	Fe/Si
1		Fe = 13.9	12.2	1633	18.9	28.4	1.66
2	Crust thickness = 62 km; density = 2.7 g/cm	Fe = 12.7	15.6	1832	24.2	30.6	1.88
3		Fe = 13.2	11.5	1633	19.2	28.2	1.64
4		Fe = 12.0	15.0	1826	24.3	30.4	1.86
5		Fe = 11.2	10.9	1631	19.4	27.1	1.53
6	Crust thickness = 38 km; density = 3.1 g/cm	Fe = 10.0	14.7	1831	24.7	29.3	1.75
7		Fe = 10.6	10.2	1629	19.6	26.9	1.52
8		Fe = 9.3	14.2	1831	25.0	29.2	1.73
9	C1 Chondrite					27.8	1.71

(1998) used the mantle composition model of [Wanke and Dreibus \(1988\)](#); (3) we use the most recent inferred mean MOI factor [Konopliv et al. \(2011\)](#) as the constraint on the 1-D density model, while [Bertka and Fei \(1998\)](#) used the [Folkner et al. \(1997\)](#) polar MOI factor; and (4) we consider the error bar of the inferred MOI factor, while [Bertka and Fei \(1998\)](#) did not.

If we adopt what [Bertka and Fei \(1998\)](#) did, but use a liquid Fe–S system in the core, we obtain a composition model of Mars that has a S content of 7.1 wt% in the core, a core radius of 1423 km, an Fe content of 25.4 wt% and an Fe/Si ratio of 1.40 (Point B in [Fig. 8](#), Line 2 in [Table 5](#)). The Fe content and the Fe/Si ratio are smaller than those of CI chondrite (Fe% = 27.8 wt%, Fe/Si = 1.71, Line 12 in [Table 3](#)), but larger than [Bertka and Fei \(1998\)](#) results (Fe% = 23.1 wt%, Fe/Si = 1.319, Line 11 in [Table 3](#)). Since liquid Fe has a smaller density than solid Fe, a liquid core assumption requires a smaller S content in the core than a solid core assumption and results in a larger Fe content and a larger Fe/Si ratio in Mars. If we consider the error bar of the [Folkner et al. \(1997\)](#) polar MOI factor observation (0.3662 ± 0.0017) and ignore the constraint of core radius, the possible Mars composition range becomes that S content in the core is between 0 and 14.3 wt%, core radius between 1262 and 1691 km, the Fe content between 24.2 and 28.4 wt%, and the Fe/Si ratio between 1.29 and 1.67 (Points A, C in [Fig. 8](#), Lines 1, 3 in [Table 5](#)). This composition range is not broad enough to encompass the composition of CI chondrite.

If we use the most recent [Konopliv et al. \(2011\)](#) mean MOI factor (0.3645 ± 0.0005) with error bars, instead of the [Folkner et al.](#)

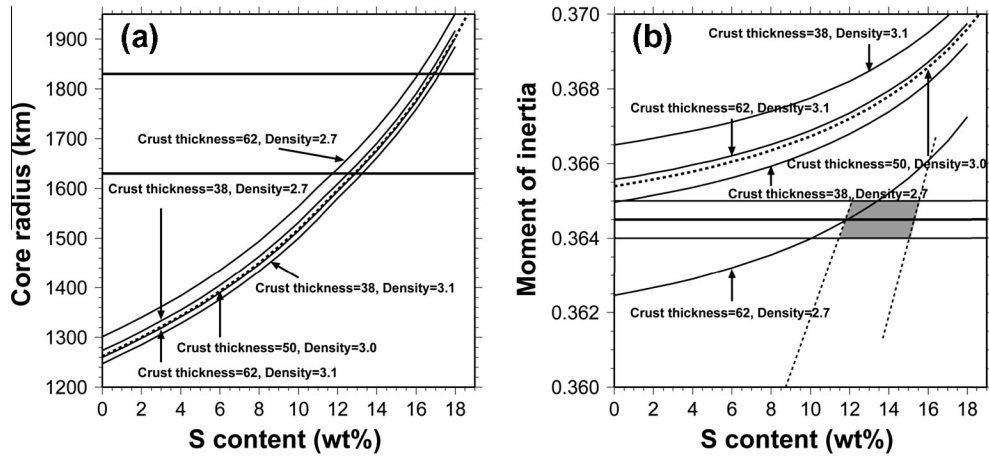


Fig. 6. Calculated core radius (a) and MOI factor (b) as a function of S content in the core for the composition model of Wanke and Dreibus (1988) in the mantle and different crustal models. The solid lines in (a) and the dashed lines in (b) are the range of possible core radius, 1630 km and 1830 km inferred by Konopliv et al. (2011); the solid lines in (b) are the observed value and error bars of the polar MOI factor.

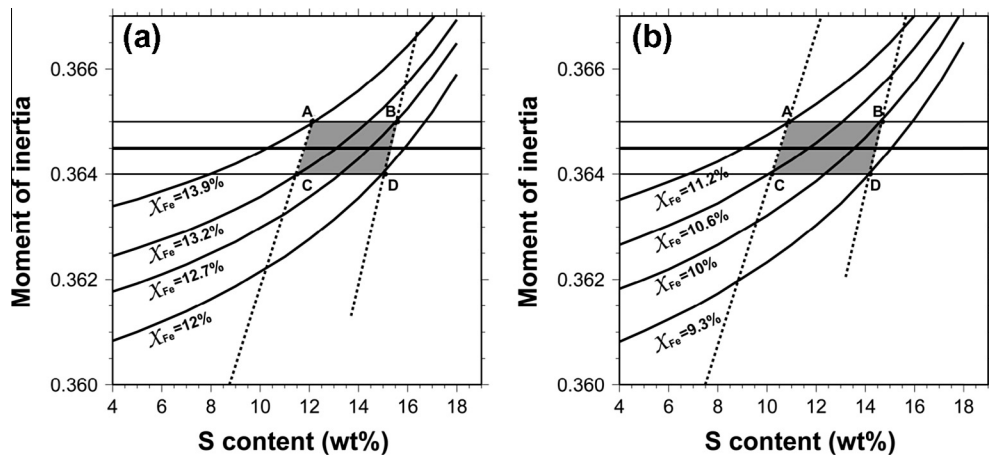


Fig. 7. Calculated MOI factor as a function of S content in the core for the composition model of Wanke and Dreibus (1988) in the mantle and two different Martian crust models: (a) with a thickness of 62 km and a density of 2.7 g/cm³; (b) with a thickness of 38 km and a density of 3.1 g/cm³. The dashed lines are the range of possible core radius, 1630 and 1830 km inferred by Konopliv et al. (2011); the solid lines are the observed value and error bars of the mean MOI factor.

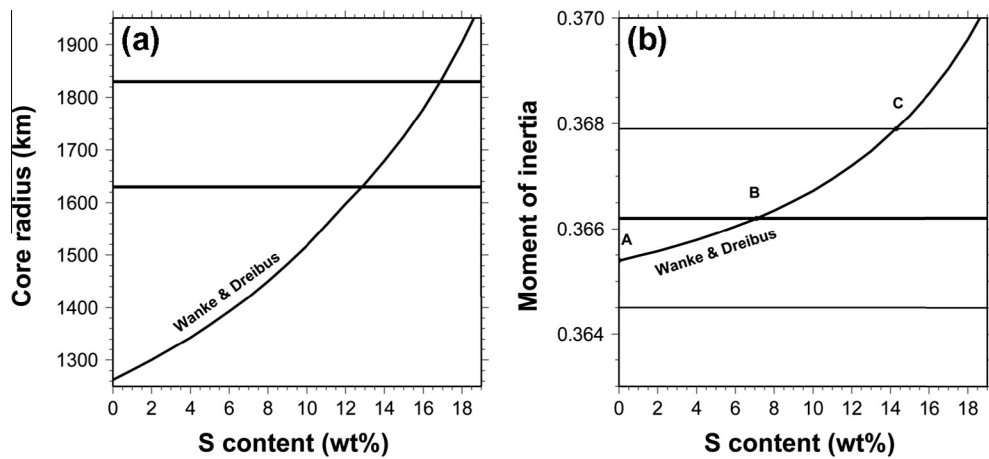


Fig. 8. Calculated core radius (a) and MOI factor (b) as a function of S content in the core for the mantle composition model of Wanke and Dreibus (1988). The solid lines in (a) and the dashed lines in (b) are the range of possible core radius, 1630 and 1830 km inferred by Konopliv et al. (2011); the solid lines in (b) are the observed value and error bars of the mean MOI factor.

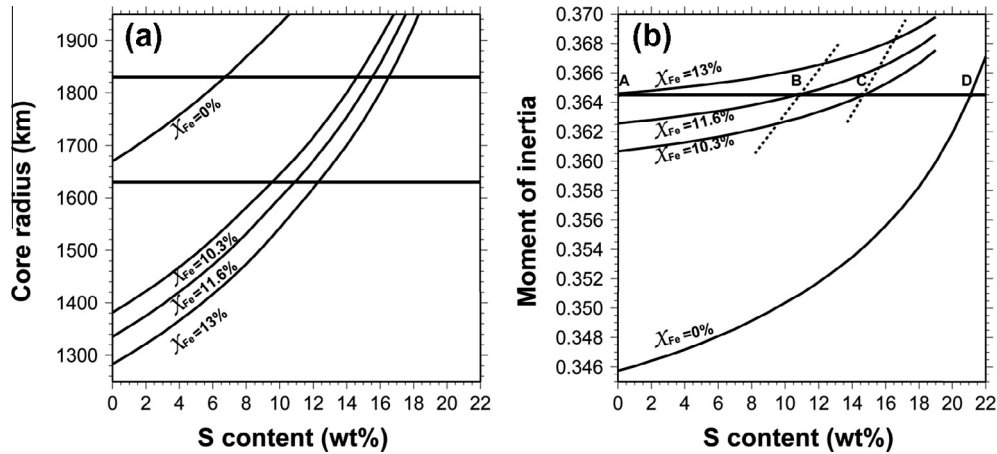


Fig. 9. Calculated core radius (a) and MOI factor (b) as a function of S content in the core for various Fe contents (X_{Fe}). The solid lines in (a) are the range of possible core radius, 1630 and 1830 km inferred by Konopliv et al. (2011); the solid lines in (b) are the observed value and error bars of the mean MOI factor.

(1997) polar MOI factor, and the fixed Wanke and Dreibus (1988) composition model in the mantle, there is no possible core composition model to fit the inferred mean MOI factor (Fig. 2). Such conclusion is still valid even if we ignore the constraint of core radius.

If we allow the mantle composition to vary, but ignore the error bar of the inferred mean MOI factor and the constraint of core radius, the inferred Fe content in the mantle is between 0 and 13 mol%, S content in the core between 0 and 21.1 wt%, core radius between 1283 and 2552 km, the Fe content between 24.3 and 41.9 wt%, and the Fe/Si ratio between 1.29 and 3.45 (Points A, D in Fig. 9, Lines 7, 10 in Table 3). The composition range is broad enough to encompass the CI chondrite composition. If we add an additional constraint of the inferred core radius (1630–1830 km, Konopliv et al., 2011), the compositional models are narrowed down to a range with Fe content in the mantle between 10.3 and 11.6 mol%, S content in the core between 10.8 and 14.6 wt%, the total Fe content between 27.3 and 29.5 wt%, and the Fe/Si ratio between 1.55 and 1.77 (Points B, C in Fig. 9, Lines 8, 9 in Table 3). This composition range is still too broad to conclude if Mars has the same bulk composition like that of CI chondrite.

Above discussions suggest that neither the liquid core assumption nor the Konopliv et al. (2011) mean MOI factor would change the conclusion that the bulk composition of Mars is different from that of CI chondrite, even if the error bars of the MOI factor is considered. But the variation of mantle composition would broaden the Mars possible composition range enough to reach the compo-

sition of CI chondrite. Even with the additional constraint of possible core radius, the composition range is still too broad to conclude if Mars has the same nonvolatile element abundances as those of CI chondrite.

Our conclusion that the possible composition range is too broad to distinguish if Mars has the same nonvolatile bulk composition as that of CI chondrite is consistent with the study of Rivoldini et al. (2011). But our inferred S content in the Martian core (10.6–14.9 wt%) is lower than what they infer (13.9–17.8 wt%). Both studies use Konopliv et al. (2011) mean MOI factor as a constraint, but Rivoldini et al. (2011) use the tidal love number k_2 as an additional constraint, while we use the inferred Martian core radius as an additional constraint. Rivoldini et al. (2011) mineralogy model did not consider the Al-bearing mineral phases, while our model does. Our mineral physics modeling shows that although Al content in the Martian mantle is low, it has significant effects on phase transformations and density distribution, and should be considered. Rivoldini et al. (2011) did not consider the chemical interactions between olivine and pyroxene components, which have significantly effects on phase transformations, while our mineral physics modeling considers not only the temperature and pressure effects but also the chemical interactions between olivine and pyroxene components.

Our inferred S content in the Martian core is consistent with the SNC meteorites analyses of Dreibus and Wanke (1985) (14 wt%) and Lodders and Fegley (1997) (10.5 wt%), but is smaller than the

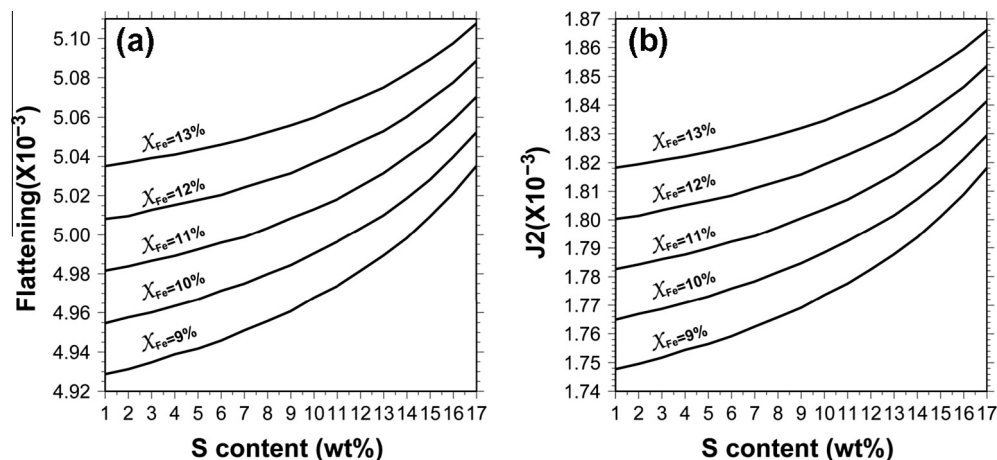


Fig. 10. Calculated flattening factor (a) and J_2 values (b) as a function of S content in the core for various Fe contents (X_{Fe}) in the mantle.

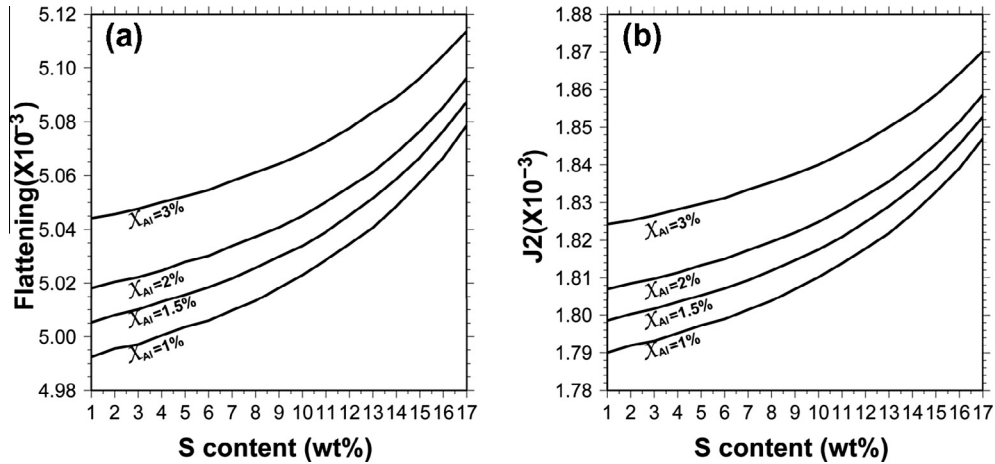


Fig. 11. Calculated flattening factor (a) and J_2 values (b) as a function of S content in the core for various Al contents (X_{Al}) in the mantle.

Table 7

J_2 and the flattening factor calculating using the second-order internal theory of equilibrium and using approximate equations.

Moment of inertia	$J_2 (\times 10^{-3})$	Approximate $J_2 (\times 10^{-3})$	$dJ_2 (\times 10^{-3})$	$f (\times 10^{-3})$	Approximate $f (\times 10^{-3})$	$df (\times 10^{-3})$
0.3641	1.8110	1.8074	0.0036	5.0243	4.9971	0.0272
0.3643	1.8134	1.8098	0.0036	5.0279	5.0007	0.0272
0.3646	1.8159	1.8137	0.0022	5.0315	5.0066	0.0249
0.3648	1.8193	1.8161	0.0032	5.0369	5.0102	0.0267
0.3650	1.8226	1.8187	0.0039	5.0419	5.0141	0.0278

studies of Sanloup et al. (1999) (16 wt%) and Mohapatra and Murty (2003) (17 wt%).

4.4. Hydrostatic flattening factor and gravitational J_2 value of Mars

The external gravitational potential of a planet is commonly described as $U = \frac{GM}{r} (1 - \sum_{n=1}^{\infty} J_{2n} P_{2n}(\sin\varphi))$, where M is the total mass, G the gravitational constant, r the radial distance, J_{2n} the numerical coefficients that describe the departure of the gravitational field from the spherical symmetry and P_{2n} the Legendre polynomials of degree $2n$. The flattening factor $f = \frac{a-b}{a}$, where a and b are the radius at the equator and the poles respectively, describes the flattening of the planet from a perfect sphere.

The observed flattening factor and J_2 value of the gravity field of Mars consist of two components, with one related to the hydrostatic figure of the rotating Mars and the other associated with the spherical harmonic degree 2 density heterogeneity in the Martian mantle. Estimate of these physical fields related to the Mars hydrostatic figure is thus important for separating the contributions of these physical fields from the density heterogeneity in the Martian mantle. We calculate the flattening factor and the J_2 value related to the hydrostatic figure of Mars based on different composition models (Figs. 10 and 11), using the second-order internal theory of equilibrium of a self-gravitating and rotating planet. We estimate the hydrostatic flattening factor to be $(5.0304 \pm 0.0098) \times 10^{-3}$ and the hydrostatic gravity J_2 value to be $(1.8151 \pm 0.0065) \times 10^{-3}$. The differences between our estimates and those estimated using approximate equations: $J_2 \approx \frac{5m}{3 \times (2.5 - 3.75C)^2 + 3} - \frac{m}{3}$ and $f \approx \frac{1}{2}(m + 3J_2)$, while $m = \frac{\omega^2 R^3}{GM}$ (Yoder and Standish, 1997) (Table 7), are 0.2–0.3% for J_2 and 0.5–0.6% for f (Table 7). In comparison with the magnitudes of non-hydro-

static values, the differences are significant for studying the density anomaly in the interior of Mars.

4.5. Non-existence of a perovskite layer in the Martian lower mantle

Whether there exists a perovskite layer in the bottom of the Martian mantle is important for understanding the generation and growth of mantle plume during the Mars thermal evolution history (Harder and Christensen, 1995; Van Thienen et al., 2006). There are three perovskite-generating phase transformations: (1) ringwoodite transforming to perovskite plus magnesiowustite, (2) garnet to perovskite and (3) garnet to ilmenite, then to perovskite. Phase transformation 3 only occurs under the condition of low temperature and/or low Al content. Phase transformations 1 and 3 are endothermic, while phase transformation 2 exothermic. The depths of these phase transformations are controlled by mantle temperature, composition and chemical interaction between olivine and pyroxene components. There are three different scenarios: (a) high mantle temperature, (b) low mantle temperature and/or low Al content without ilmenite, and (c) low mantle temperature and/or low Al content with ilmenite. In scenario a, in the absence of chemical interaction between olivine and pyroxene systems, phase transformation 1 occurs at a pressure lower than phase transformation 2. However, because of some partitioning of Al from garnet to the ringwoodite-transforming perovskite and the reduced Al content in the garnet system deriving phase transformation 2, two phase transformations occur at a same depth controlled by the endothermic phase transformation 1 (Wang et al., 2006). In this scenario, the perovskite-forming depth is controlled by mantle temperature. For example, increasing mantle temperature by 100 K would result in a 10-km shallower perovskite layer. For the Fei and Bertka (2005) temperature model and Wanke and

Dreibus (1988) compositional model or models with our possible mantle Fe contents, the depth of the phase transformations is 1800 km, requiring a core radius smaller than 1590 km for a perovskite layer to exist. Konopliv et al. (2011) inferred that Martian core radius is between 1630 and 1830 km. So existence of a perovskite layer in the bottom of the Martian mantle would require a Martian mantle temperature at least 400 K higher than Fei and Bertka (2005) temperature model, which would reach the mantle solidus and become unreasonable. In scenario b, phase transformation 2 occurs at a pressure lower than phase transformation 1 and the temperature and/or Al content is not low enough for ilmenite phase to appear. In this scenario, the emerging depth of a perovskite layer is dominant by phase transformation 2, which is controlled by the Al content and mantle temperature. A lower Al content and/or a lower mantle temperature would result in a smaller perovskite-forming depth, and vice versa. In scenario c, the perovskite-forming depth is controlled by phase transformation 3 (Wang et al., 2006), which is sensitive to mantle temperature. A lower mantle temperature would result in a larger perovskite-forming depth, and vice versa. For all the possible temperatures and Al contents that would make the perovskite-forming transformations under scenarios b or c, the smallest perovskite-forming depth is 1760 km, which would require a core radius smaller than 1620 km, beyond the inferred Martian core radius range (1630–1830 km) by Konopliv et al. (2011). We thus conclude that no perovskite layer exists in the bottom of Martian mantle.

5. Conclusions

We calculate density profiles in Mars for various mantle compositions, core compositions and a liquid core assumption. We then calculate the MOI factors of Mars and compare them with the observation to place constraints on Mars composition. With the constraints of the total mass, possible core radius and the inferred mean MOI factor, we find that Fe content in the Martian mantle is between 9.9 and 11.9 mol%, Al content in the Martian mantle smaller than 1.5 mol%, S content in the Martian core between 10.6 and 14.9 wt%, the total Fe content in Mars between 27.3 and 32.0 wt%, and the Fe/Si ratio in Mars between 1.55 and 1.95. The inferred composition range is too broad to make a conclusion if Mars has the same nonvolatile bulk composition as that of CI chondrite. With our reference crust model, Wanke and Dreibus (1988) composition model is not a plausible mantle composition model for Mars, but a thicker or less dense crust can make it plausible. We estimate the flattening factor and the J_2 value related to the hydrostatic figure of Mars to be $(5.0304 \pm 0.0098) \times 10^{-3}$ and $(1.8151 \pm 0.0065) \times 10^{-3}$ respectively, based on various inferred compositions of the planet, using the second-order internal theory of the equilibrium of a self-gravitating and rotating planet. In our possible Martian composition range, it is unlikely for a perovskite layer to exist in the bottom of the Martian mantle.

Acknowledgements

This work is supported by a CNSF Grant #41104035 and Chinese Academy of Sciences/State Administration of Foreign Experts Affairs International Partnership Program for Creative Research Teams.

References

- Allegre, C., Manhès, G., Lewin, E., 2001. Chemical composition of the Earth and the volatility control on planetary genetics. *Earth Planet. Sci. Lett.* 185, 49–69.
- Anderson, D.L., 1972. Internal constitution of Mars. *J. Geophys. Res.* 77, 789–795.
- Anderson, W.W., Ahrens, T.J., 1994. An equation of state for liquid-iron and implications for the Earth's core. *J. Geophys. Res.* 99, 4273–4284.
- Balog, P.S., Secco, R.A., Rubie, D.C., Frost, D.J., 2003. Equation of state of liquid Fe–10 wt% S: implications for the metallic cores of planetary bodies. *J. Geophys. Res.* 108. <http://dx.doi.org/10.1029/2001JB001646>.
- Bertka, C.M., Fei, Y., 1998. Implications of Mars Pathfinder data for the accretion history of the terrestrial planets. *Science* 281, 1838–1840.
- Birch, F., 1947. Finite elastic strain of cubic crystals. *Phys. Rev.* 71, 809–824.
- Dreibus, G., Wanke, H., 1985. Mars, a volatile-rich planet. *Meteoritics* 20, 367–381.
- Fei, Y., Bertka, C.M., 2005. The interior of Mars. *Science* 308, 1120–1121.
- Folkner, W.M., Yoder, C.F., Yuan, D.N., Standish, E.M., Preston, R.A., 1997. Interior structure and seasonal mass redistribution of Mars from radio tracking of Mars Pathfinder. *Science* 278, 1749–1752.
- Ganapathy, R., Anders, E., 1974. Bulk composition of the Moon and Earth, estimated from meteorites. *Fifth Luna Sci. Conf.* 2, 1181–1206.
- Gasparik, T., 1990. Phase relations in the transition zone. *J. Geophys. Res.* 95, 15751–15769.
- Gasparik, T., 2003. Phase diagrams for geoscientists, An atlas of the Earth's interior. Springer, Verlag Berlin, Heidelberg, New York.
- Harder, H., Christensen, U., 1995. A one-plume model of Martian mantle convection. *Nature* 380, 507–509.
- Javoy, M., Kaminski, E., Guyot, F., Andrault, D., Sanloup, C., Moreira, M., Labrosse, S., Jambon, A., Agrinier, P., Davaile, A., Jaupart, C., 2010. The chemical composition of the Earth: enstatite chondrite models. *Earth Planet. Sci. Lett.* 293, 259–268.
- Konopliv, A.S., Asmar, S.W., Folkner, W.M., Karatekin, O., Nunes, D.C., Smrekar, S.E., Yoder, C.F., Zuber, M.T., 2011. Mars high resolution gravity fields from MRO, Mars seasonal gravity, and other dynamical parameters. *Icarus* 211, 401–428.
- Lodders, K., Fegley, B.J.R., 1997. An oxygen isotope model for the composition of Mars. *Icarus* 126, 373–394.
- Mocquet, A., Vacher, P., Grasset, O., Sotin, C., 1996. Theoretical seismic models of Mars: the importance of the iron content of the mantle. *Planet. Space Sci.* 44, 1251–1268.
- Mohapatra, R.K., Murty, S.V.S., 2003. Precursors of Mars: constraints from nitrogen and oxygen isotopic compositions of Martian meteorites. *Meteorit. Planet. Sci.* 38, 225–241.
- Ringwood, A.E., 1959. On the chemical evolution and densities of the planets. *Geochim. Cosmochim. Acta* 15, 257–283.
- Rivoldini, A., Van Hoolst, T., Verhoeven, O., Mocquet, A., Dehant, V., 2011. Geodesy constraints on the interior structure and composition of Mars. *Icarus* 213, 451–472.
- Sanloup, C., Jambon, A., Gillet, P., 1999. A simple chondritic model of Mars. *Phys. Earth Planet. Inter.* 112, 43–54.
- Sanloup, C., Guyot, F., Gillet, P., Fiquet, G., Mezouar, M., Martinez, I., 2000. Density measurements of liquid Fe–S alloys at high-pressure. *Geophys. Res. Lett.* 27, 811–814.
- Urey, H.C., 1952. *The Planets: Their Origin and Development*. Yale University Press, New Haven, CT.
- Van Thienen, P., Rivoldini, A., Van Hoolst, T., 2006. A top-down origin for Martian mantle plumes. *Icarus* 185, 197–210.
- Wang, Y., Wen, L., Weidner, D.J., He, Y., 2006. SH velocity and compositional models near the 660-km discontinuity beneath South America and northeast Asia. *J. Geophys. Res.* 111, doi: 10.1029/2005JB003849.
- Wang, Y., Wen, L., Weidner, D.J., 2008. Upper mantle SH- and P-velocity structures and compositional models beneath southern Africa. *Earth Planet. Sci. Lett.* 267, 596–608.
- Wang, Y., Wen, L., Weidner, D.J., 2009. Array triplication data constraining seismic structure and composition in the mantle. *Surv. Geophys.* <http://dx.doi.org/10.1007/s10712-009-9073-3>.
- Wanke, H., Dreibus, G., 1988. Chemical-composition and accretion history of terrestrial planets. *Philos. Trans. R. Soc. Lond. Ser. A* 325, 545–557.
- Weidner, D.J., Wang, Y., 1998. Chemical- and Clapeyron-induced buoyancy at the 660 km discontinuity. *J. Geophys. Res.* 103, 7431–7441.
- Wieczorek, M.A., Zuber, M.T., 2004. Thickness of the Martian crust: improved constraints from geoid-to-topography ratios. *J. Geophys. Res.* 109. <http://dx.doi.org/10.1029/2003JE002153>.
- Yoder, C.F., Standish, E.M., 1997. Martian precession and rotation from Viking lander range data. *J. Geophys. Res.* 102, 4065–4080.
- Yoder, C.F., Konopliv, A.S., Yuan, D.N., Standish, E.M., Folkner, W.M., 2003. Fluid core size of Mars from detection of the solar tide. *Science* 300, 299–303.